A Hybrid Tensor Factorization - Singular Spectrum Analysis Approach for ERP-based Assessment of Autism in Children

Beatriz Sanabria-Barradas
Centro de Investigaciones Biomédicas
Universidad Veracruzana
Xalapa, Veracruz, México
beti.sanabria0121@gmail.com

Saeid Sanei
Department of Computer Science
Nottingham Trent University
Nottingham, UK
saeid.sanei@ntu.ac.uk

Dora E. Granados-Ramos
Laboratorio de Psicobiología
Universidad Veracruzana
Xalapa, Veracruz, México
dgranados@uv.mx

***Abstract*—Diagnosis of autism spectrum disorder (ASD) in children is often achieved by estimating the amplitudes and latencies of visual event-related potentials (ERPs). This requires accurate detection of desired ERPs, in our case P1 and N170, which are sensitive to visual stimuli. We aim to develop a hybrid of tensor factorization (TF) and singular spectrum analysis (SSA) to detect these components from electroencephalograms (EEGs) and restore the inherent noise and artifacts. The application of single-channel SSA to the detected sources by TF results in the removal of brain beta activity considerably enhancing the accuracy. The ERP parameters (amplitudes and latencies) are automatically estimated and applied to a decision-tree classifier leading to 100% accuracy.**

***Index Terms*—Autism Spectrum Disorder, Decision Tree, EEG, Emotions, Event-Related Potentials, Singular Spectrum Analysis, Tensor Decomposition**

I. Introduction

Electroencephalography (EEG) is a neurophysiological functional screening technique that records brain electrical activity in real-time and non-invasively. Each EEG electrode signal is the sum of a large number of neuronal sources, modeled as dipoles, emitted from the cortex and other brain zones [1]–[4]. These signals are often contaminated by wide-band noise, blinking and movement artifacts, and in our case, undesired cortical activities. Therefore, it is essential to preprocess the EEG signals before continuing with their analysis. Although methods such as blind source separation are effective in removing EEG artifacts, there are often undesired sources that are correlated (or overlap) with the desired ones in space, time, or frequency [5], [6].

One of the topics that have received major attention in characterizing the EEG is the event-related potentials (ERPs). Their research includes face processing, mainly for a developmental approach to studying disorders such as Autism Spectrum Disorder (ASD). This is a neurodevelopmental disorder characterized by the presence of behavioral alterations, including qualitative impairment in social interactions, language, and communication, as well as a restricted range of activities presented with repetitive and stereotyped patterns [7], [8].

ASD individuals show deficits in face perception owing to abnormal face processing strategies caused by perceptual abnormalities, such as a locally oriented rather than global visual analysis, or more complex alterations of the social brain network. Further, the impaired face perception in ASD individuals could also underpin social interaction difficulties [9].

Due to this, the main ERPs used to study the face processing disability in ASD individuals are P1 and N170 since they are related to visual stimuli. The P1 component is a positive deflection located in occipital areas that reaches its maximum peak around 100 ms approximately. It reflects systematic differences to any visual stimulus, whether faces or objects [10]. The N170 component is a negative deflection recorded from electrodes over the occipital-temporal cortex that peaks at approximately 170 milliseconds and are better observed in adults [11]. Also, this component has been used as a marker for the specialized neural and perceptual mechanisms associated with the early stages of face processing, recognition, and identification of faces resulting from visual stimuli [12]–[15].

In some studies, it has been reported that the latency and amplitude of both ERPs, P1, and N170, decrease with age. This is mainly, in control children of 3 to 5 years old. For these children, the latency can increase from 260 to 291 ms and the amplitude decrease from -6 to -5 μV [16]. In children of 6 to 9 years old the latency and amplitude vary respectively from 200 to 250 ms and -6 to 1 μV. In children from 10 to 11 years of age, they vary respectively from 180 to 250 ms and from -3 to -2 μV. Finally, in adolescents from 12 to 15 years old, these change respectively from 160 to 200 ms and from -7 to -3 μV [16]–[19]. These values have been estimated using face and object recognition tasks. Also, during such trials, it has been documented that the control children, faced with faces rotated 180°, have longer latency in their N170 and P1 components. However, in ASD children this pattern has not been observed, but the N170 latencies are longer than those in control children [16]–[20].

In terms of data classification, some studies have tried to find EEG features for diagnosing ASD based on emotions or

resting state. They are using mainly the power spectral density (PSD) and multiscale entropy (mMSE). Applying different classifiers such as artificial neural network (ANN), support vector machines (SVM), random forest machine, K-contractive map (K-CM), and k-nearest neighbors (KNN), they have obtained accuracies between 87.3 and 92.8% [21], [22].

In the following, we propose a method based on singular spectrum analysis (SSA) to remove beta rhythm due to attention and tensor decomposition to separate and characterize the ERPs from the rest of the independent artifacts, such as blink eye, motion, or noise. Furthermore, we demonstrate how to select the components and calculate the ERP parameters and the most discriminating features for the classification of autistic and control. We organize the paper as follows: In section II, we give a brief introduction to SSA and tensor decomposition. In section III, we describe our approach to automatic selection of components and the features extraction related to the ERPs, including the experimental setup, and finally discuss the results in section IV.

II. SSA and Tensor decomposition

A. SSA

SSA is a nonparametric technique that decomposes a time series into a set of summable components that can be grouped and interpreted by their trend, periodicity, and noise. Mainly, it emphasizes the separability of the underlying components, since periodicities occurring on different time scales can be easily separated, even in very noisy time-series data. This means the original time series is recovered by adding all its components, therefore, it can be used to analyze and reconstruct a time series with different components while rejecting the undesired components [23]–[26].

The SSA consists of four steps, the first two related to the decomposition and the last ones to the reconstruction. The first one constitutes the construction of the trajectory matrix. Let $F = (f_0, f_1, ..., f_{N-1})$ be a time series of length N, and L be an integer, the window length. We set $K = N - L + 1$ and define the L-lagged vectors $X_j = (f_{j-1}, ..., f_{j+L-2})^T$, $j = 1, 2, ..., K$, and the trajectory matrix, well known as Hankel matrix $X = (f_{i+j-2})_{i,j=1}^{L}, K = [X_1 : ... : X_K]$.

The second step is the singular value decomposition (SVD) of the matrix X, which can be obtained via eigenvalues and eigenvectors of the matrix $S = XX^T$ of size $L \times L$. With this, we obtain a representation of X as a sum of rank-one biorthogonal matrices $X_i (i = 1, ..., d)$, where $d (d \leq L)$ is the number of nonzero singular values of X. Projecting the time series onto the direction of each eigenvector yields the corresponding temporal principal component (PC).

In the third step, we split the set of indices $I = 1, ..., d$ into groups $I_1, ..., I_m$ and sum the matrices X_i within each group, obtaining: $X = \sum_{k_1}^{m} X_{I_k}$, where $X_{I_k} = \sum_{i \epsilon I_k} X_i$. Finally, in the fourth step, we perform the averaging over the diagonals $i + j = \text{const}$ of the matrices X_{I_k}, giving an SSA decomposition, which is a decomposition of the original series F into a sum of series $f_n = \sum_{k=1}^{m} f_n^{(k)}, n = 0, ..., N-1$, where for each k the series $f_n^{(k)}$ is the result of diagonal averaging of the matrix X_{I_k} [23], [24], [26].

Considering that each eigenvalue is equal to the variance of the signal in the direction of the corresponding PC, only the largest eigenvalues belong to the signal and the smallest to the noise [24]. Also, in the eigenvalue pattern, any two equal size adjacent eigenvalues represent a periodic component in the mixed signal. To filter our time signal, we discard all the PCs that correspond to eigenvalues beyond 95% of the total variance of the signal. Eigenvalue λ_i is selected if i is less than L:

$$L = \arg\min_a \left\{ \frac{\sum_{i=1}^{a} \lambda_i}{\sum_{i=1}^{l} \lambda_i} > 0.95 \right\} \quad (1)$$

Then, we remove the undesired beta frequency component together with other artifacts by detecting its corresponding pair of equal amplitude eigenvalues.

B. Tensor Decomposition

A tensor is an extension of a higher-order matrix that can be indexed by an arbitrary number of indices. According to this, the goal of tensor decomposition is to obtain a compact representation of the tensor. There are mainly two types of tensor decompositions, CANDECOMP/PARAFAC (CP) and Tucker, which can be considered higher-order generalizations of matrix singular value decomposition (SVD) and principal component analysis (PCA). The idea of CP decomposition is to convert the tensor into a sum of rank-one components, while the Tucker decomposition can be viewed as a generalization of the CP decomposition, where the core matrix is not para-diagonal. However, Tucker decomposes the tensor into a small core tensor and factorial matrices, thus generating a core tensor with the same order as the original tensor and a list of projection matrices, one for each mode of the original tensor. Nevertheless, the CP decomposition is the most frequently employed decomposition technique mainly because the solution is unique. For a three-dimensional tensor, the CP model is defined as:

$$\chi \approx \sum_{r=1}^{R} a_r \circ b_r \circ c_r \quad (2)$$

where $\circ$ is the outer product R is the rank of the model, quantifiying the latent features extracted, and a_i, b_i, c_i are the three loading vectors (Fig. 1) [27], [28].

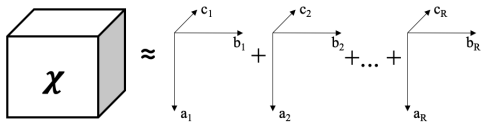

Fig. 1. The principle of CP decomposition for a three-dimensional tensor [27], [28].

The disadvantage of CP decomposition is the need for a priori information on the decomposition rank R, however, this can be set equal to the number of expected components (factors) in the signal, in our case, equal to 4. In the following,

we will therefore introduce an approach to automatically remove motion artifacts from the EEG and select the ERP components based on readily measurable signal statistical characteristics.

III. Algorithm

We aim to characterize the EEG signal of children with ASD through an emotion test. Because of this, we apply CP decomposition to extract ERP-related features, SSA to remove the undesired brain activities and artifacts and find the amplitude and latency measures of P1 and N170. Fig. 2 depicts the entire process which is done automatically as explained in more detail below.

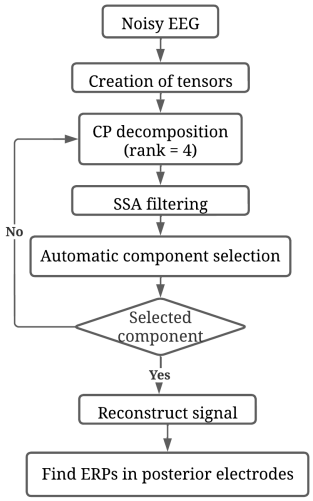

Fig. 2. Framework for the estimation of ERPs using CP decomposition and SSA method.

A. Experimental setup and data acquisition

We used the SynAmps RT to record 180s data at 1000 Hz sampling frequency from eight children, four with ASD and four healthy while attending an emotion test that contains 128 visual stimuli, 64 faces, and 64 balls. Each stimulus lasted 850 ms and between each of them, there was a fixation cross with a duration of 866.66 ms (Fig. 3). The test was shown individually in a silent room while 19 electrodes were located according to the 10-20 standard electrode placement system. This test protocol was evaluated by an ethics committee and was approved with the number CONBIOÉTICA 30CE100120180131, also the parents and children signed informed consent.

B. Tensorization

Before applying CP decomposition, EEG needs to be transformed into a tensor. In the first step, we grouped the round and oval faces and did the same for the objects. Then, we created epochs per stimulus considering 100 ms previous and 500 ms after it, obtaining 128 epochs in total. With this information, a three-dimensional tensor was created for faces

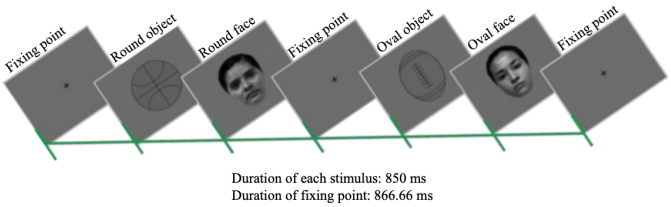

Fig. 3. Emotion test. Presentation scheme and duration of stimuli for ERP N170. (Data from the Laboratorio de Psicobiología).

and objects and was made up of the dimensions: *channel, time, and trial* (Fig. 4). With that, the CP decomposition can explore spatial, temporal, and spectral (across trials) correlations in the data to find the ERPs features.

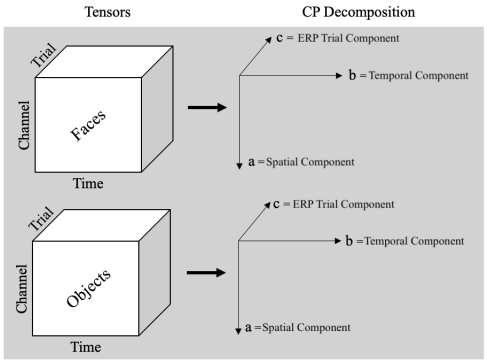

Fig. 4. Tensorization: constructing a tensor per stimulus, considering 64 trials, 19 channels and times from -100 ms to 500 ms.

C. Filtering

Major contributors of artifacts most detected in EEG recording are eye movement-related artifacts, cardiac signals, the tension of the facial, jaw, or body muscles, and body movement. These signals have a frequency range of around 0.5-40 Hz, making it difficult to separate them from our signal of interest because of spectral overlap [29].

All independent or disjoint artifacts such as noise, eye blinks, and muscle artifacts are removed from multichannel EEGs by tensor factorization in a similar way to independent component analysis. After the CP decomposition, we used the SSA method to remove the beta activity due to attention and remaining artifacts from the time components. Considering that an appropriate window length L is a compromise between computational cost and decomposition quality, and each column vector of the trajectory matrix has to include at least one cycle of the periodic source with the lowest frequency of interest, the lower bound for L is 50 and we set $L = 100$ so that two cycles of each existing periodic components are included.

D. Automatic selection of components and signal reconstruction

Knowing that our ERPs of interest are generated in the posterior brain area and have a specific signature, we design

an algorithm to select the component automatically. For this purpose, to verify that the component is in the posterior area we select the spatial components of P3, P4, T5, T6, O1, and O2 electrodes and calculated the mean value per component. All components that have a mean value higher than zero are added to a vector (SEs). To find the signature related to the ERPs, P1, and N170, we select the segment from 70 to 350 ms of all temporal components and search for the max and min values per each one. The same as in the previous criterion, the number of components that have their max value between 70 and 175 ms and their amplitudes are higher than $15\mu V$ are added to a vector (Smax), and those with their min value between 180 and 350 ms, and an amplitude lower than -21 μV to another vector (Smin). The only component selected is the one that meets all the three criteria (Fig. 5).

Considering the uniqueness of CP decomposition, we multiply the time and spatial component arrays and choose the selected component in the previous step to visualize the ERPs in the channels of interest (Fig. 6). Also, we find the amplitude and latency of P1 and N170 automatically in the last stage.

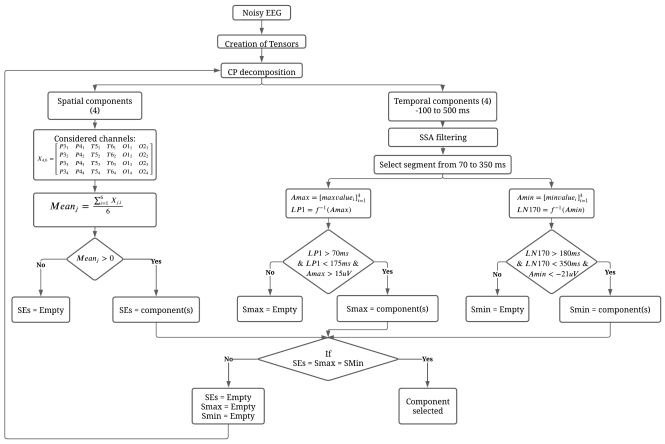

Fig. 5. Automatic ERP selection algorithm.

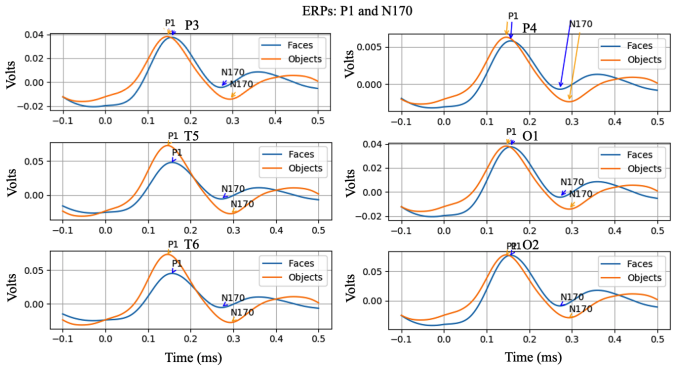

Fig. 6. Example of ERPs calculated for a control child.

IV. Results

Fig. 7 clearly shows the low efficiency of the conventional band-pass filter (0.5 - 50 Hz) in removing the beta band signal superimposed on the the signal, which did not allow an accurate selection of the ERPs, and consequently a comparison of the classifiers could not be made. Conversely, in the same figure, the effectiveness of SSA can be observed, which allows a more accurate selection of the ERPs and parameter estimation. Then, using the SSA, we combine all the cases per group and calculate the amplitude and latency of P1 and N170 for each electrode (P3, P4, T5, T6, O1, and O2). Also, we evaluate both measures per hemisphere obtaining 33 attributes related to faces and 33 to objects, 66 attributes in total. Table I illustrates the results of our proposed method. Although no statistically significant differences were found between groups, we observed that the latency of P1 and N170 in ASD children is less for faces and more for objects than in control children and demonstrated no differences in response between the two brain hemispheres. However, in terms of amplitude, ASD children showed higher values when visualized faces and lower for objects in P1, and lower values in N170, mainly in the right hemisphere for both stimuli. In addition, control children showed higher P1 amplitude in the right hemisphere for faces and to objects in the left hemisphere, and lower N170 amplitudes in the left hemisphere for faces and the right hemisphere for objects.

With this information, we evaluate the performance of the decision tree classifier to identify an ASD case with the ERPs. When using the 66 attributes, faces, and objects, we obtained only 33% of correctly classified instances. However, with the 33 object attributes, we achieved 100% accuracy.

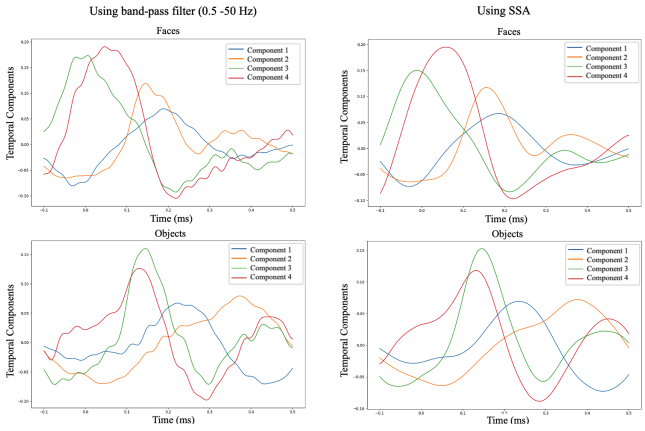

Fig. 7. Filtering: basic filtering and SSA method compare

V. Conclusion

Traditionally, The EEGs are averaged over trails for ERP detection. This ignores the ERP variability for different trials. In this work, we have proposed to use the CANDECOMP/PARAFAC (CP) decomposition to extract features related to the ERPs. Besides, we found that the SSA method as a powerful single-channel decomposition technique can completely remove the effect of beta frequency due to attention. The combination of these two approaches allows for more accurate ERP detection and automation of autism diagnosis.

TABLE I
P1 AND N170 ERPS RELATED TO FACES AND OBJECTS PER ELECTRODE.

Group	Stimuli	Electrodes	ERPs			
			P1		N170	
			Amp (μV)	*Lat (ms)*	*Amp (μV)*	*Lat (ms)*
ASD	Faces	O1	43.4	135.5	-19.1	260.8
		O2	48.3		-19.2	
		T5	39.1		-19.8	
		T6	44.6		-19.5	
		P3	18.8		-16.8	
		P4	27.6		-17.8	
	Objects	O1	23.2	119.5	-29.1	234.0
		O2	28.0		-31.9	
		T5	15.7		-26.6	
		T6	26.1		-31.4	
		P3	3.1		-17.6	
		P4	14.5		-23.4	
Control	Faces	O1	32.5	122.3	-12.1	244.0
		O2	42.1		-12.2	
		T5	30.1		-15.2	
		T6	29.7		-8.8	
		P3	11.6		-6.3	
		P4	15.8		-6.3	
	Objects	O1	53.9	131.0	-16.6	248.3
		O2	44.6		-17.6	
		T5	40.2		-15.0	
		T6	28.2		-14.5	
		P3	11.8		-8.4	
		P4	12.6		-9.8	

Amp: Amplitude, *Lat:* Latency.

Even with the limited number of cases in our study, our results coincide with those reported in other studies.

In terms of classification, a decision-tree classifier was selected due to the diversity in the number of features for different subjects and different stimuli obtaining a good accuracy. However, nonlinear classifiers, such as deep learning methods may cater to even more diverse applications. In comparison with other approaches in autism classification, stated in the Introduction section, our approach outperforms the existing techniques.

ACKNOWLEDGMENT

To the Consejo Nacional de Ciencia y Tecnología (CONACYT) that has contributed with the PhD Scholarship No. 717999.

REFERENCES

[1] S. Sanei and J. A. Chambers, "EEG Signal Processing and Machine Learning", UK: Wiley, 2021.
[2] E. Niedermeyer, "Electroencephalography. Basic Principles, Clinical Applications And Related Fields", USA: Wolters Kluwer, 2011.
[3] R. M. Rangayyan, "Biomedical Signal Analysis", Canada: IEEE Press, 2015.
[4] K. Whittingstall. G. Stroink, L. Gates, J. F. Connolly and A. Finley, "Effects of dipole position, orientation and noise on the accuracy of EEG source localization", BioMedical Engineering OnLine, vol. 2, pp. 1–5, 2003.
[5] M. Klados, C. Papadelis, C. Braun and P. D. Bamidis, "REG-ICA: a hybrid methodology combining blind source separation and regression techniques for the rejection of ocular artifacts", Biomedical Signal Processing and Control, vol. 6, pp. 291–300, 2011.
[6] G. L. Wallstrom, R. E. Kass, A. Miller, J. F. Cohn and N. A. Fox, "Automatic correction of ocular artifacts in the EEG: a comparison of regression-based and component-based methods", International Journal of Psychophysiology, vol. 53, pp. 105–119, 2004.
[7] American Psychiatric Association, "Diagnostic and Statistical Manual of Mental Disorders (DSM-5)", 5th ed., Washington: Panamericana, 2014.
[8] R. Calderón-González and R. F. Calderón-Sepúlveda, "Polemic or controversial therapies in the neurodevelopmental disorders", Rev Neurol, vol. 31, pp. 368–375, 2000.
[9] C. Costa, I. A. Cristea, E. Dal Bo, C. Melloni and C. Gentili, "Brain activity during facial processing in autism spectrum disorder: an activation likelihood estimation (ALE) meta-analysis of neuroimaging studies", Journal of Child Psychology and Psychiatry, pp. 1–13, 2021.
[10] D. Kuefner, A. Heering, C. Jacques, E. Palmero-Soler and B. Rossion, "Early visually evoked electrophysiological responses over the human brain (P1, N170) show stable patterns of face-sensitivity from 4 years to adulthood", Frontiers in Human Neuroscience, vol. 3, pp. 1–22, 2010.
[11] S. Bentin, T. Allison, A. Puce, E. Perez and G. McCarthy, "Electrophysiological studies of face perception in humans", Journal of Cognitive Neuroscience, vol. 8, pp. 551—565, 1996.
[12] D. Anaki, E. Zion-Golumbic and S. Bentin, "Electrophysiological neural mechanisms for detection, configural analysis and recognition of faces", NeuroImage, vol. 37, pp. 1407–1416, 2007.
[13] A. V. Flevaris, L. C. Robertson and S. Bentin, "Using spatial frequency scales for processing face features and face configuration: an ERP analysis", Brain Research, vol. 1194, pp. 100–109, 2008.
[14] V. Macchi Cassia, A. Westerlund, D. Kuefner and C. A. Nelson, "Modulation of face-sensitive event-related potentials by canonical and distorted human faces: the role of two visual structural properties", Journal of Cognitive Neuroscience, vol. 18, pp. 1343–1358, 2006.
[15] J. W. Tanaka and T. Curran, "A neural basis for expert object recognition", Psychological Science, vol. 12, pp. 43–47, 2001.
[16] M. J. Taylor, G. E. Edmonds, G. McCarthy and T. Allison, "Eyes first! Eye processing develops before face processing in children", Cognitive Neuroscience and Neuropsychology, vol. 12, pp. 1671–1676, 2001.
[17] M. J. Taylor, G. McCarthy, E. Saliba and E. Degiovanni, "ERP evidence of developmental changes in processing of faces", Clinical Neurophysiology, vol. 110, pp. 910–915, 1999.
[18] C. Tye, E. Mercure, K. L. Ashwood, B. Azadi, P. Asherson, M. H. Johnson, P. Bolton and G. McLoughlin, "Neurophysiological responses to faces and gaze direction differentiate children with ASD, ADHD and ASD + ADHD", Developmental Cognitive Neuroscience, vol. 5, pp. 71–85, 2013.
[19] R. Tsurusawa, Y. Goto, A. Nakashima and S. Tobimatsu, "Different perceptual sensitivities for Chernoff's face between children and adults", Neuroscience Research, vol. 60, pp. 176–183, 2008.
[20] C. M. Hileman, H. Henderson, P. Mundy, L. Newell and M. Jaime, "Developmental and individual differences on the P1 and N170 ERP components in children with and without autism", Developmental Neuropsychology, vol. 36, pp. 214–236, 2011.
[21] N. F. Harun, N. Hamzah, N. Zaini, M. M. Sani, H. Norhazman and I. M. Yassin, "EEG classification analysis for diagnosing autism spectrum disorder based on emotions", Journal of Telecommunication, Electronic and Computer Engineering, vol. 10, pp. 87–93, 2018.
[22] B. Deepa and K. S. Jeen Marseline, "Exploration of autism spectrum disorder using classification algorithms", Procedia Computer Science, vol. 165, 2019.
[23] N. Golyandina, V. Nekrutkin and A. A. Zhigijavsky, "Analysis of Time Series Structure: SSA and Related Techniques", USA: Chapman and Hall/CRC, 2001.
[24] J. Mamou and E. J. Feleppa, "Singular spectrum analysis applied to ultrasonic detection and imaging of brachytherapy seeds", Journal of the Acoustical Society of America, vol. 121, pp. 1790–1801, 2009.
[25] W. C. A. Pereira, S. L. Bridal, A. Coron and P. Laugier, "Singular spectrum analysis applied to backscattered ultrasound signals from in vitro human cancellous bone specimens", IEEE Transactions on Ultrasonics, Ferroelectrics, and Frequency Control, vol. 51, pp. 302–312, 2004.
[26] T. J. Harris and H. Yuan, "Filtering and frequency interpretations of singular spectrum analysis", Physica D, Nonlinear Phenom, vol. 239, pp. 1958–1967, 2010.
[27] T. G. Kolda and B. W. Bader, "Tensor decompositions and applications", Society for Industrial and Applied Mathematics Review, vol. 51, pp. 455–500, 2009.
[28] N. D. Sidiropoulos, L. De Lathauwer, X. Fu, K. Huang, E. E. Papalexakis and C. Faloutsos, "Tensor decomposition for signal processing and machine learning", IEEE Transactions on Signal Processing, vol. 65, pp. 3551–3582, 2017.
[29] J. N. Knight, "Signal fraction analysis and artifact removal in EEG", Master's thesis, Department Comput. Sci., Colorado State Univ., 2003.